



FSI MODELING OF LIQUID SLOSHING IN A FLEXIBLE FLOATING TANK UNDER REGULAR WAVE EFFECT

GHOUINI F.^{1,2,}, KHA K.Q.N.^{2,3}, BENAOUICHA M.^{2,3}, SEGHIR A.¹,
GUILLOU S.², SANTA CRUZ A.²*

¹ Research Laboratory of Applied Hydraulics and Environment, Faculty of Technology, University of Bejaia, Targa Ouzemmour, 06000 Bejaia, Algeria

² University of Caen Normandie, LUSAC, EA 4253, Normandy University, 60 Street Max Pol Fouchet, CS 20082, 50130 Cherbourg-Octeville, France

³ Segula Technologies, Naval and Energy Engineering Research and Innovation Unit, 9 Avenue Edouard Belin, 92500 Rueil-Malmaison, France

(**) fatiha.ghouini@univ-bejaia.dz*

Research Article – Available at <http://larhyss.net/ojs/index.php/larhyss/index>
Received May 22, 2024, Received in revised form August 25, 2024, Accepted August 28, 2024

ABSTRACT

This paper presents a Fluid-Structure Interaction (FSI) numerical study of a deformable two-dimensional floating rectangular tank partially filled with water and subjected to a regular wave effect. It is based on the coupling of a two-phase flow solver from the OpenFOAM code, based on the Finite Volume Method (FVM), and an elastic solid solver from the FEniCS code, based on the Finite Element Method (FEM). The two solvers are coupled using the preCICE library for the Fluid-Structure Interaction (FSI) problem. The Arbitrary Lagrangian-Eulerian (ALE) formulation is adopted for the two-phase Navier-Stokes equations in a moving fluid domain. An implicit coupling scheme is used to solve the FSI problem. The effect of swell excitation is considered by introducing a source term into the equations governing the fluid and the solid. The obtained results show that for the studied case, the tank walls' flexibility increases the sloshing amplitude and the fluctuations at the air-liquid interface, and causes a phase shift in the free surface response compared to the rigid case. The Fast Fourier Transform (FFT) applied to the time responses of the free surface and the tank wall highlights that the obtained results give a good agreement with the analytical solution.

Keywords: FSI coupling, Numerical modeling, Regular waves, Sloshing, Deformable tank, Floating tank.

INTRODUCTION

Numerous tanks serve the purpose of either storing or transporting liquids (Bahloul Guerbabi and Farhi, 2015). These vary from the transportation of liquid energy, such as vehicle fuel to tanks designed for non-energy liquid products like drinking water. In instances where the tank is not completely filled and exposed to complex external excitations, the sloshing phenomenon occurs. In summary, sloshing in tanks can contribute to tank deterioration when combined with other factors like deformations and displacements of tank walls. Proper design, material selection, and maintenance practices are crucial to ensuring the longevity and safety of storage tanks. On the flip side, floating systems for marine renewable energies, including floating tidal and wind turbines, represent innovative and promising solutions for harnessing clean energy from the ocean (Debbache and Derfouf, 2018). Using a partially filled liquid is one method to enhance the stability of floating structures, particularly for floating wind turbines. The key principle involves using a water-filled structure with a significant portion submerged below the waterline.

The investigation of sloshing has recently become increasingly popular. A numerical model was developed by Liu et al. (2020) to investigate the behavior of the liquid oxygen inside a tank subjected to sinusoidal excitation considering various parameters such as sloshing force, moment, pressure, and dynamic response of the free interface. The results obtained are validated by existing experimental data. They highlight the influence of density, damping effects, and external excitation on various parameters within the system. An experimental approach was used to study sloshing under combined heave and sway motions using an experimental approach, while a numerical approach was used to analyze sloshing under combined heave and surge motions (Jin et al., 2022). The numerical study presents the influence of surge frequency on sloshing pressure due to unstable heave excitation. Cases of off-resonant surge frequencies show less violent peak dynamic pressures, while near-resonant or resonant frequencies exhibit significant increases in peak dynamic pressure. Using the bidirectional coupling method, Luo et al. (2022) investigated the height of sloshing waves in storage tanks after seismic excitation. The research emphasized the critical importance of choosing suitable numerical methods to ensure precise estimation of sloshing peak values. The study further underscored the imperative for customized seismic design considerations, particularly in the specific context of large-scale LNG storage tanks situated in regions prone to seismic activity. The sloshing dynamics were studied by Kargbo et al. (2021) by examining the interaction between oil and water and a T-shaped baffle in a rectangular tank that was subjected to pitching excitation. The investigation employed a combination of numerical simulations and experimental setups to investigate sloshing phenomena in tanks, considering factors like mesh convergence, layered sloshing, interaction with porous structures, and the effects of T-shaped porous baffles on fluid behavior. The results demonstrated good agreement between experiments and numerical simulations. An experimental study on the parametric sloshing behavior in a tank subjected to high-frequency and low-frequency excitation conducted by Yu et al. (2019) was carried out on a six-degree-of-freedom motion platform, and the focus was on understanding how vertical baffles influence parametric sloshing (Yu et al., 2020a). The findings suggest that the optimal number and

position of baffles depend on the specific sloshing mode and provide valuable information for designing effective damping strategies in practical applications. A numerical and an experimental investigations were conducted by Akyildiz and Ünal (2005), Akyildiz and Erdem Ünal (2006) that focused on pressure distributions at various locations and the three-dimensional effects on liquid sloshing within a partially filled 3D rectangular tank subjected to pitch oscillations. The study explored multiple configurations, including both baffled and unbaffled tanks. The comparisons reveal good agreement for both impact and non-impact slosh loads in the investigated cases. Faltinsen (1974) developed a third-order steady-state solution for liquid sloshing in a two-dimensional rectangular tank. This solution is applicable when the tank is excited by swaying and rolling motions. This solution is based on Moiseev's theory (Moiseev, 1958). A numerical methodology based on a cell-centered pressure-based algorithm and the level set method was developed in (Chung-Yueh Wang et al., 2010) to determine the sloshing motion of fluid in a two-dimensional rectangular tank, incorporating either a single baffle or two baffles. Validation of the numerical results is performed against published data, particularly from Armenio (1997), demonstrating good agreement. Yu et al. (2020b) analyzed a violent liquid sloshing in a rigid cylindrical tank equipped with multiple rigid annular baffles and provoked by an external excitation with either large amplitudes or resonant frequencies. the study demonstrates the significant impact of impermeable and permeable baffles on sloshing behavior, providing insights into the optimal design parameters for suppressing sloshing in liquid cargo transport systems.

The earlier-mentioned studies did not explore the impact of flexibility on the sloshing behavior of the liquid under varying excitations, nor did they consider the Fluid-Structure Interaction (FSI) effects. The numerical interaction between liquid sloshing and an elastic and rigid baffle was studied by Ren et al. (2023) using SPHinXsys. The obtained results are validated with the experiments. The liquid sloshing behavior in a flexible tank subjected to external excitation was analyzed by Khouf et al.(2023) using a two-phase flow solver and an elastic solid solver within the OpenFOAM code by taking into account Fluid-Structure Interaction (FSI) effects. The model is utilized to evaluate the impact of liquid sloshing on the tank's dynamic response and the influence of tank flexibility on liquid sloshing. The analysis reveals that the proposed model obtains excellent results, validated against analytical solutions for linear sloshing and experimental data for nonlinear sloshing. The Finite Volume Method of OpenFOAM has not provided an accurate solution to the structure equation. A new numerical coupling model was proposed by Kha et al. (2024) for investigating the sloshing dynamics in a 2D flexible rectangular tank under complex excitation, coupling OpenFOAM code and FEniCS code through the preCICE coupling library to investigate the influence of varying liquid filling levels in a flexible tank under seismic excitation. The proposed coupling model proves reliable and efficient for studying sloshing in a flexible tank subjected to external excitation.

Despite the abundance of literature on sloshing, there are no studies dealing with sloshing in a floating flexible tank exposed to the swell effect. This research aims to develop a numerical model by coupling a two-phase flow solver within the OpenFOAM code using the Finite Volume Method (FVM) and an elastic solid solver within the FEniCS code

using the Finite Element Method (FEM). This coupling is facilitated through the preCICE coupling library. To study the effect of wall flexibility on liquid sloshing a partially filled tank subjected to swell excitation is considered. In this study, the tank is completely carried by the free surface. The structure of this paper is outlined as follows. Section 2 describes the problem, including the parameters of the swell excitation. Following that, Section 3 covers the mathematical modeling and numerical model, while Section 4 explores the effects of swell excitation on liquid sloshing within a flexible tank. Lastly, Section 5 summarizes and concludes the study.

PROBLEM DESCRIPTION AND PARAMETERS

In this study, our emphasis is on the storage tanks within a marine vessel (Figure 1). Specifically, a partially filled 2D rectangular floating deformable tank with a length $L_s = 0.57m$ and a height $H_s = 0.3m$. The tank is filled to 50% ($H_f = 0.15m$) capacity with water and is subjected to motion driven by waves. The tank walls thickness is determined to be $t_w = 0.02m$. (All the tank's dimensions are reduced with a 1/40 scale.)

The swell is treated as a regular wave characterized by a peak-to-valley height, $h_{pv} = 0.15m$. It is modeled as a periodic oscillatory motion of the water surface, with a period, $T_p = 12s$, obtained from equation (2). This period represents the time interval between two consecutive wave peaks or two successive wave valleys at a specific point situated on the water surface at rest. The wavelength, $\lambda = 5.7m$, represents the horizontal distance between two corresponding points on two successive wave peaks or wave valleys, obtained with the ratio $\lambda = 10 L_s$ corresponding to the real value $\lambda = 228m$ (see all parameters in Figure 1). The period (T_p) plays a crucial role in determining the morphology of oceanic waves and has a significant impact on their length and frequency, as noted by Molin (2002). Commencing with the period equation (equation (1)), we can derive the relationship for the wavelength (equation (2)).

$$T_p = \sqrt{\frac{2\pi\lambda}{g}} \quad (1)$$

$$\lambda = 1.56 T_p^2 \quad (2)$$

The dynamic behavior of both the tank and the liquid inside is represented through a coupling of the OpenFOAM code for fluid dynamics, employing the finite volume method, and the FEniCS code for structural dynamics, utilizing the finite element method (Amara et al., 2013a; 2013b; 2016; Amara and Berreksi, 2018). This coupling is achieved using the preCICE library. In this analysis, the influence of waves is entirely dictated by the modified gravity (as indicated in equation (4)). This gravitational effect is incorporated as a source term in both the fluid and structure equations (9) and **Erreur ! Source du renvoi introuvable.** respectively. All calculations are conducted within the reference frame of the tank.

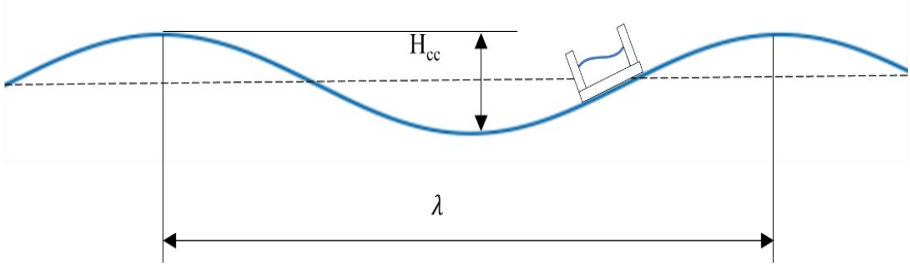


Figure 1: Tank motion in a seaway.

NUMERICAL MODEL

In this study, the waves and the swell of interest are exclusively influenced by gravity. We consider that the floating reservoir follows the motion of the wave. The basis associated with the reservoir is the origin of the reference system $(o\vec{x}_1 \vec{y}_1)$ located at the center of the tank and at the free surface at rest ($\eta = 0$). Causing a tilting of the reservoir within the reference system $(o\vec{x}_1 \vec{y}_1)$ to the reference system $(o\vec{x}_0 \vec{y}_0)$ located at the center of the tank and the free surface elevation with an inclination angle α , as defined by equation (3).

To facilitate the simulation in this reference system $(o\vec{x}_0 \vec{y}_0)$, (see Figure 2), the conventional gravitational force, denoted as \vec{g} , was replaced with an acceleration attributed to the waves, represented by \vec{A}_s . It is expressed according to equation (4) in the basis $(o\vec{x}_1 \vec{y}_1)$ linked to the reservoir.

$$\alpha = \alpha_{max} \cos(\omega t) \quad (3)$$

$$\vec{A}_s = \vec{g}_s + \vec{\gamma}_e \quad (4)$$

Here, \vec{g}_s represents the gravity influenced by the waves expressed by $\vec{g}_s = g \sin(\alpha) \vec{x}_1 + g \cos(\alpha) \vec{y}_1$, while $\vec{\gamma}_e$ denotes the rotational maintenance due to the water's rotation, α_{max} is the maximal angle of inclination given by equation (5), ω is the angular frequency (equation (6)), t is the time, and \vec{x}_1 , \vec{y}_1 are the unit vectors in terms of positive directions of axes (x_1) and (y_1) respectively,.

$$\alpha_{max} = \tan^{-1}(2h_{cc}/\lambda) \quad (5)$$

$$\omega = 2\pi/T_p \quad (6)$$

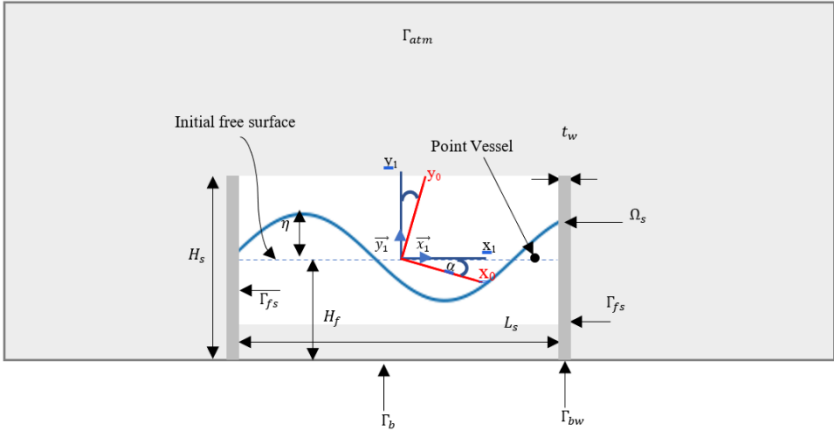


Figure 2: Diagram presenting the case study.

Figure 3 shows the curves of the various components of equation (4). For a first approximation, the tank is considered to be a materially small point in relation to the swell, resulting in a wavelength larger than the reservoir's length, which prevents rotation due to water. Under this approximation, the rotation effect is neglected thus that equation (4) becomes equation (7) as follows:

$$\vec{g}_s = g \sin(\alpha) \vec{x}_1 + g \cos(\alpha) \vec{y}_1 \tag{7}$$

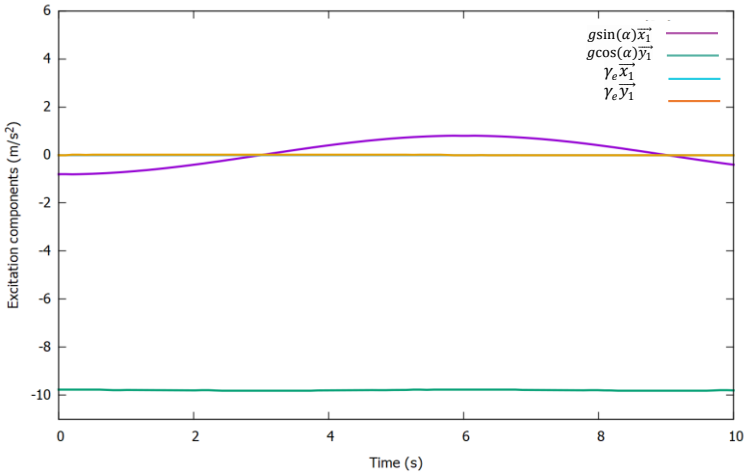


Figure 3: Presentation of different components of the applied excitation.

Fluid dynamics

The analysis of fluid dynamics within the tank involves resolving the Navier-Stokes equations for an incompressible two-phase fluid (Lebdiri et al., 2020). Given that the fluid moves alongside a container in motion, adjustments to the motion equation are necessary to incorporate the displacement of the domain. The expression of the Navier-Stokes equations in moving domain is facilitated through the utilization of the Arbitrary Lagrangian-Eulerian formulation (Ozdemir et al., 2009). The derivation of these equations involves a combination of the continuity equation (8) and the momentum equation (9):

$$\nabla \cdot \vec{u} = 0 \quad (8)$$

$$\rho_f \frac{\partial \vec{u}}{\partial t} + \rho_f ((\vec{u} - \vec{w}) \cdot \nabla) \vec{u} = -\nabla P + \mu_f \Delta \vec{u} + \rho_f \vec{g}_s + \vec{f}_\sigma \quad (9)$$

Where: ρ_f is the density of the fluid mass, \vec{u} is the flow velocity, w is the domain displacements velocity, P is the fluid pressure, μ_f is the kinematic viscosity of the two-phase (liquid and air), and \vec{f}_σ is the surface tension (at the air-water interface).

Equation (10) gives the fluid issue's boundary and initial conditions. Where: $\vec{\xi}$ is the structural velocity, n is the normal unitary vector to the open top boundary Γ_{atm} , Γ_b is the bottom boundary, Γ_{fs} is the fluid-structure interface, and Ω_f is the fluid domain.

$$\begin{cases} \frac{\partial \vec{u}}{\partial n} = 0 & \text{on } \Gamma_{atm} \\ \vec{u} = 0 & \text{on } \Gamma_b \\ \vec{u} = \vec{\xi} & \text{on } \Gamma_{fs} \\ \vec{u}(0) = 0 & \text{on } \Omega_f \end{cases} \quad (10)$$

In OpenFOAM, the Volume of Fluid method (VOF) is employed to handle two-phase flows involving two immiscible fluids with no inter-phase exchange. This approach was used in this study for modeling and monitoring fluid interface. The volume fraction ψ ($0 \leq \psi \leq 1$) is employed to signify the proportion or rate of volume occupied by the liquid within a specific cell. The function ψ is advected with the velocity field u , according to equation **Erreur ! Source du renvoi introuvable.**

$$\frac{\partial \psi}{\partial t} + \nabla \cdot \vec{u} \psi + \nabla \cdot \vec{u}_r (\psi(1 - \psi)) = 0 \quad (11)$$

$\vec{u}_r = \vec{u}_l - \vec{u}_g$ is the relative velocity of the liquid relative to air. u_l and u_g are respectively the velocities of the liquid and the gas. This artificial term is introduced to restrict the diffusion of the air-liquid interface.

The fluid density and the dynamic viscosity are given by:

$$\rho_f = \rho_l \psi + \rho_g (1 - \psi) \quad (11)$$

$$\mu_f = \mu_l \psi + \mu_g (1 - \psi) \tag{12}$$

Where the indices l et g represent the liquid phase and the gas phase respectively.

In OpenFOAM, the Finite Volume Method (FVM) is employed to discretize the equations governing the two-phase flow.

Structure dynamics

The structure deformations are determined by the linear elasticity equation (13), wherein $\vec{\xi}$ represents the local displacement field, σ_s is the stress tensor (14) within the structure, ρ_s is the structure mass density, and the gravity vector \vec{g}_s , defined by equation (4), is furthermore a contributing factor.

$$\rho_s \frac{\partial^2 \vec{\xi}}{\partial t^2} = \nabla \cdot \sigma_s + \rho_s \vec{g}_s \tag{13}$$

with:

$$\sigma_s = \lambda_s tr(\epsilon) I + 2\mu_s \epsilon \tag{14}$$

$$\epsilon = 1/2 (\nabla \xi + \nabla^T \xi) \tag{15}$$

$$\begin{cases} \lambda_s = \frac{\nu_s E}{(1+\nu_s)(1-2\nu_s)} \\ \mu_s = \frac{E}{2(1+\nu_s)} \end{cases} \tag{16}$$

Where λ_s and μ_s are Coefficients of Lamé of the structure, ϵ represents the strain tensor, E is the young coefficient and ν_s is Poisson's ratio.

The boundary conditions and initial conditions for the structure problem are provided by the relations (17) where Γ_{bw} is the wall limit, Ω_s is the solid domain, σ_f is the stress tensor in the fluid and n is the outward normal vector at the interface Γ_{fs} .

$$\begin{cases} \vec{\xi} = 0 & \text{on } \Gamma_{bw} \\ \sigma_s \cdot \vec{n} = \sigma_f \cdot \vec{n} & \text{on } \Gamma_{fs} \\ \vec{\xi}(0) = 0 & \text{on } \Omega_s \end{cases} \tag{17}$$

FEniCS uses the finite element method (FEM) for solving transport equations in structure analysis.

Fluid-structure coupling

When examining sloshing inside a flexible tank, it is crucial to incorporate Fluid-Structure Interaction (FSI) phenomena (Messaudène and Ferrouk, 2024). This can be effectively tackled through the application of diverse coupling techniques (Rajaomazava et al., 2011). The coupling between fluid and structure involves equations that describe the

interaction and influence of one on the other. Thus, the velocity and stress continuity must be satisfied at the fluid-structure interface (equation (18)).

$$\begin{cases} \vec{u} = \vec{\xi} & \text{on } \Gamma_{fs} \\ \sigma_s \cdot \vec{n} = \sigma_f \cdot \vec{n} & \text{on } \Gamma_{fs} \end{cases} \quad (18)$$

In this study, the partitioned method is used, coupling OpenFOAM and FEniCS via preCICE with an implicit scheme algorithm. This involves the resolution of fluid equations through OpenFOAM and structure equations through FEniCS. After meeting a predefined convergence criterion, it becomes essential to iterate through this process multiple times within each time step. The preCICE interface ensures the exchange of data between the two software codes. The numerical model was validated by the simulation of a rigid and flexible tank exposed to harmonic excitation comparing with experimental data and analytical predictions.

SLOSHING UNDER WAVE EFFECTS

To investigate the influence of the flexibility of the tank walls on liquid sloshing dynamics, two distinct cases involving tanks made of different materials are examined. A rigid reservoir with a Young's modulus of $E = 15 \cdot 10^{20} \text{ MPa}$ and a flexible one with a Young's modulus of $E = 15 \text{ MPa}$ are considered. In both cases, the same tank is considered without any external excitation (under hydrostatic pressure effect). In the flexible tank case, only the gravity force causes the deformation of the walls until approaches a stable value of maximum deflection, as depicted in Figure 4. The computed value is 5.1 mm , approximately matching the analytical value $d_a = 5.59 \text{ mm}$ calculated using the formula (20) of the beam theory where H_f is the fluid filling level, H_s is the walls height, E is the Young's modulus, and I is the quadratic moment of inertia of the beam's cross section. The relative difference between the two values is approximately 8.77%.

$$d_a = \frac{\rho_f g H_f^4}{120 E I} (5H_s - H_s) \quad (20)$$

The fluid's free surface exhibits the behavior depicted in Figure 5. After a few seconds, the free surface decreases by approximately 0.8 mm from its initial level due to deflections of both walls in opposite directions. To initiate the applied excitation case, the initial condition will be set based on this stable state, aiming to prevent fluctuations at the beginning of the simulation. Then the swell effect is applied.

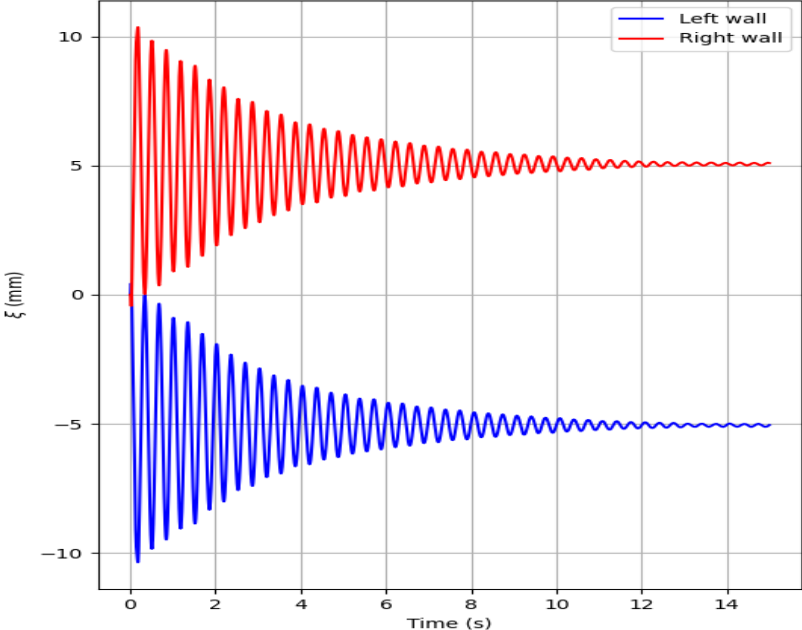


Figure 4: Displacement of the top walls in time's function.

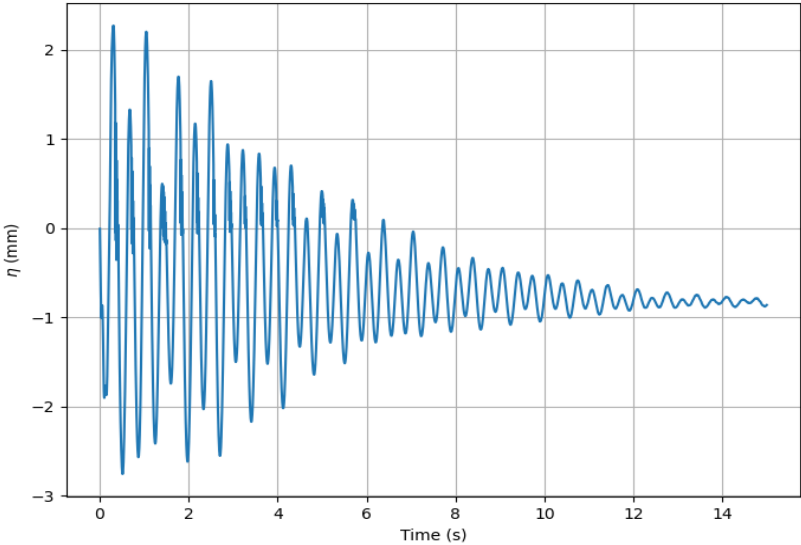


Figure 5: Free surface elevation of liquid.

Figure 6 illustrates the variations in the free surface elevation of a liquid of both flexible and rigid wall cases over time extracted at a probe located 20mm from the right wall. The data was collected at every 1s, and the resulting plot offers insights into the dynamic behavior of the liquid surface. The general trend of the graph shows that fluctuations in the free surface elevation of the flexible and rigid walls have almost the same peaks. Several prominent peaks can be observed in the results. These peaks represent the case where the free surface elevation reaches its maximum height. In addition to peaks, there are identifiable troughs where the free surface elevation reaches its lowest points. These troughs may indicate periods of decreased elevation or settling of the liquid. The maximum sloshing amplitudes are 20.85mm at $t = 6.31s$ for the flexible case and 20.49mm at $t = 6.13s$ for the rigid case, indicating an almost 1.73% difference between the two cases. A phase shift is moreover clearly observed between both cases since the flexible case is more compliant than the rigid case. This means that the flexible case can deform more readily in response to the waves generated by the excitation. The period of the modulated wave envelope $T_f = 10.73s$ is longer in the flexible tank case than in the rigid case $T_r = 10.41s$ which corresponds to 2.98% of difference.

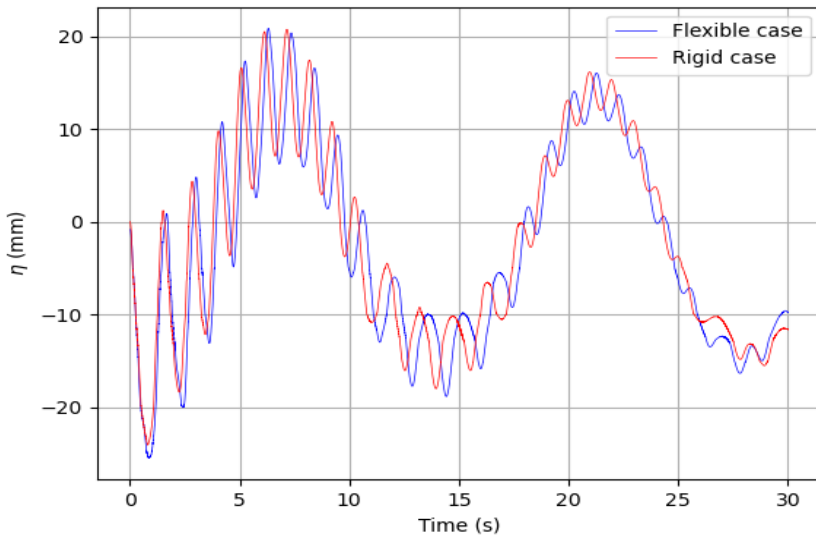


Figure 6: Free surface elevations for both flexible and rigid walls.

Figure 7 represents the tank wall deflections extracted from the points at the top of the left and right tank walls over time, measured at regular time steps. This analysis aims to understand the dynamic behavior of the wall in response to the wave effect and liquid sloshing. Figure 7 exhibits a gradual increase and then a decrease in wall displacements over the swell period. This suggests an ongoing and cumulative effect on the structural integrity of the walls. during the gradual trend, there are peaks in wall displacements. These peaks indicate the case of maximum displacement.

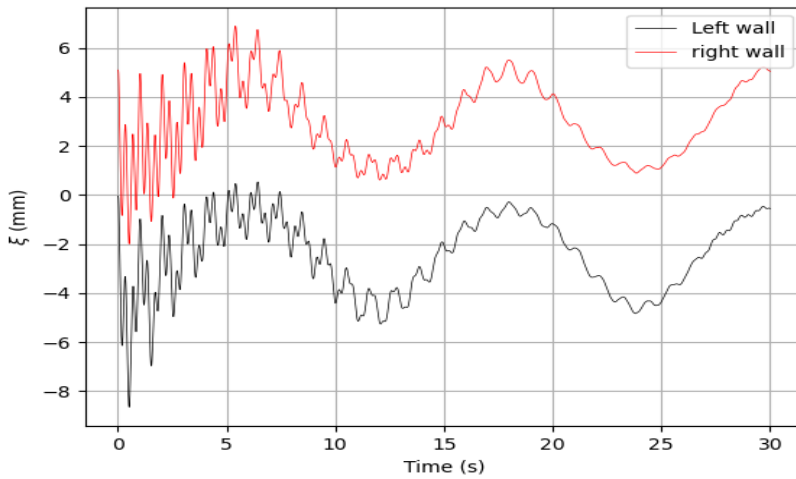


Figure 7: Top tank wall displacements.

In order to estimate the natural frequencies of a fluid and a structure, the Fast Fourier Transform (FFT) analysis is performed on the time history responses of both free surface elevations and wall displacements. Figure 8 displays the FFT curves that were acquired. Thus, the computed value of the excitation frequency ($f_{e,c} = 0.50 \text{ Hz}$) presents the first peak for both rigid and flexible walls cases which is close to the given value ($f_e = 0.52 \text{ Hz}$) with a relative difference of 3.84 %. The second peak $f_{1,c} = 0.93 \text{ Hz}$ presents the computed value of the natural sloshing frequency which is close to the analytical value $f_1 = 0.96 \text{ Hz}$ calculated from (Faltinsen and Timokha, 2009) with a difference of 3.12%. The last peak ($f_{s,c} = 1.50 \text{ Hz}$) is the computed value of the structure eigenfrequency, which are comparable to the analytical value $f_s = 1.55 \text{ Hz}$ computed from (Blevins, 2001) with a difference of 3.22%. The FFT generated many other frequencies, among these frequencies there is the frequency 3.10 Hz which corresponds to $2f_s$. Overall, the FFT analysis appears to have been successful in estimating the natural frequencies of the fluid and the structure. The computed values are close to the analytical values, with differences of less than 4%.

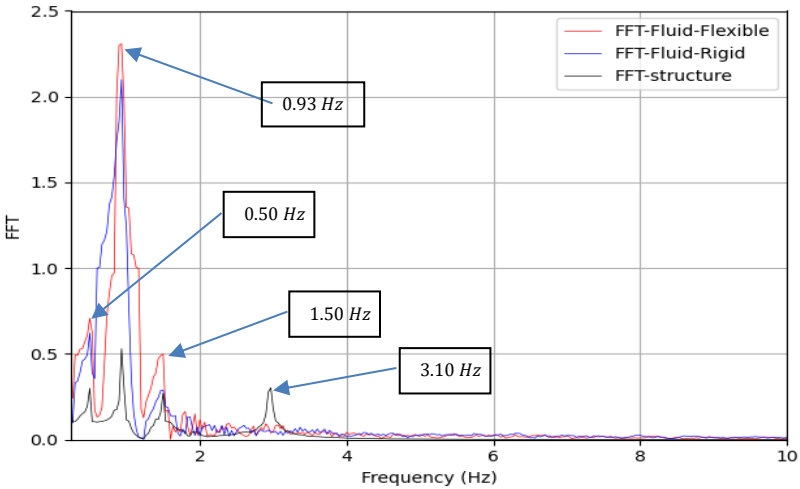


Figure 8: FFT of free surface and the wall displacement.

CONCLUSION

A numerical study on the behavior of the liquid into a two-dimensional flexible rectangular reservoir subjected to the effects of a regular swell was considered. The coupling of a two-phase flow solver in OpenFOAM with an elastic solid solver in the FEniCS code was achieved using the preCICE coupling library to model the fluid-structure interaction (FSI) problems. The Finite Volume Method (FVM) is used in OpenFOAM to discretize the two-phase flow equations. FEniCS uses the finite element method to solve the linear-elastic equation of a structure. The FSI coupling problem is solved by using an implicit coupling scheme strategy to ensure simulations stability. The numerical model was validated through comparison with analytical predictions and experimental data on a rigid and flexible tank under harmonic excitation.

The analysis of the effects of regular wave on flexible tank mentioned that the flexibility of the wall has an important effect how sloshing occurs and vice versa. It is shown that in the current study case, the influence of flexibility is not very significant, which is attributed to the fact that the swell applied is longer than the tank's size. In addition, the flexibility caused a phase shift in the free surface response between both cases that shows an important modification of the sloshing in the reservoir with a flexible wall. The FFT study showed that the obtained results are in good agreement with the analytical solution for both flexible and rigid case. This work will be extended to a 2D application of a floating reservoir into a wave channel.

Declaration of competing interest

The authors declare that they have no known competing financial interests or personal relationships that could have appeared to influence the work reported in this paper.

Acknowledgments

The present work is a part of the CUVE project with a collaboration between SEGULA Technologies, LUSAC laboratory (university of Caen, Normandy, France), and LRHAE laboratory (University of Bejaia, Algeria), within the international Cotutelle Thesis.

REFERENCES

- AKYILDIZ H., ÜNAL E. (2005). Experimental investigation of pressure distribution on a rectangular tank due to the liquid sloshing, *Ocean Engineering*, Vol.32, Issues 11-12, pp. 1503–1516.
- AKYILDIZ H., ERDEM ÜNAL N. (2006). Sloshing in a three-dimensional rectangular tank: Numerical simulation and experimental validation, *Ocean Engineering*, Vol.33, Issue 16, pp. 2135–2149.
- AMARA L., ACHOUR B., BERREKSI A. (2013a). Finite volumes numerical approach for the calculation of the dynamic response of equilibrium chimneys, *Larhyss Journal*, No 14, pp. 7-19. (In French)
- AMARA L., BERREKSI A., ABDOUNE K. (2013b). Computation of mass oscillations in a surge tank by finite element technique, *Larhyss Journal*, No 15, pp. 139-149.
- AMARA L., BERREKSI A., ACHOUR B. (2016). Application of the finite volume method to the computation of water hammer protection, *Larhyss Journal*, No 28, pp. 303-317.
- AMARA L., BERREKSI A. (2018). Computation of 1d side weir flow by finite element method, *Larhyss Journal*, No 35, pp. 45-58.
- ARMENIO V. (1997). An improved mac method (simac) for unsteady high-reynolds free surface flows, *International Journal for Numerical Methods in Fluids*, Vol.24, Issue 2, pp. 185–214.
- BAHLOUL GUERBABI F.Z., FARHI A. (2015). Water management in Timgad from the source to the ancient thermal spas, *Larhyss Journal*, No 23, pp. 259-273. (In French)
- BLEVINS R.D. (2001). *Flow-induced Vibration*, Krieger Publishing Company, 477 p.
- DEBBACHE M., DERFOUF S. (2018). Analysis of the induction effect on the performance of wind turbine, *Larhyss Journal*, No 33, pp. 25-39.

- FALTINSEN O.M. (1974). A Nonlinear Theory of Sloshing in Rectangular Tanks. *Journal of Ship Research*, Vol.18, Issue 4, pp. 224–241.
- FALTINSEN O.M., TIMOKHA A.N. (2009). *Sloshing*, Cambridge University Press, 606p.
- JIN X., LUO M., XUE M.A., LIN P. (2022). Resonant sloshing in a rectangular tank under coupled heave and surge excitations, *Applied Ocean Research*, Vol.121, Paper ID 103076.
- KARGBO O., XUE M.A., ZHENG J., YUAN X. (2021). Multiphase sloshing dynamics of a two-layered fluid and interfacial wave interaction with a porous T-shaped baffle in a tank, *Ocean Engineering*, Vol.229, Paper ID 108664.
- KHA K.Q.N., BENAOUICHA M., GUILLOU S., SEGHIR A. (2024). Numerical Investigation of Liquid Sloshing in 2D Flexible Tanks Subjected to Complex External Loading, *Journal of Fluids and Structures*, Vol.125, Paper ID 104077.
- KHOUF L., BENAOUICHA M., SEGHIR A., GUILLOU S. (2023). Numerical modeling of liquid sloshing in flexible tank with FSI approach, *World Journal of Engineering*, Vol.20, Issue 1, pp. 131–142.
- LEBDIRI F., SEGHIR A., BERREKSI A. (2020). Steps number effect on hydraulic parameters of flows in stepped spillways, *Larhyss Journal*, No 42, pp. 41–51.
- LIU Z., FENG Y., LIU Y., LEI G., LI Y. (2020). Fluid sloshing dynamic performance in a fuel storage tank under sinusoidal excitations, *Applied Thermal Engineering*, Vol.168, Paper ID 114814.
- LUO D., LIU C., SUN J., CUI L., WANG Z. (2022). Sloshing effect analysis of liquid storage tank under seismic excitation, *Structures*, Vol.43, pp. 40–58.
- MESSAOUDENE B., FERROUK M. (2024). Fluid-structure interaction with viscoelasticity in numerical simulation of water hammer, *Larhyss Journal*, No 58, pp. 7–19.
- MOISEEV N.N. (1958). On the theory of nonlinear vibrations of a liquid of finite volume, *Journal of Applied Mathematics and Mechanics*, Vol.22, Issue 5, pp. 860–872.
- MOLIN B. (2002). *Hydrodynamique des structures offshore*, Editions TECHNIP, 415 p. (In French)
- OZDEMIR Z., MOATAMEDI M., FAHJANY.M., SOULI M. (2009). ALE and Fluid Structure Interaction for Sloshing Analysis, *The International Journal of Multiphysics*, Vol.3, Issue 3, pp. 307–336.
- RAJAOMAZAVA T.E., BENAOUICHA M., ASTOLFI J.A. (2011). A Comparison Study of Coupling Algorithms for Fluid-Structure Interaction Problems, in: Vol. 4, *Fluid-Structure Interaction*. Presented at the ASME 2011 Pressure Vessels and Piping Conference, ASMEDC, Baltimore, Maryland, USA, pp. 399–408.

- REN Y., KHAYYER A., LIN P., HU X. (2023). Numerical modeling of sloshing flow interaction with an elastic baffle using SPHinXsys, *Ocean Engineering*, Vol. 267, Paper ID 113110.
- WANG C.Y., TENG J.T., HUANG G.P.G. (2010). Numerical Simulation of Sloshing Motion inside a Two-Dimensional Rectangular Tank with a Baffle or Baffles, *Journal of Aeronautics, Astronautics and Aviation. Series A*, Vol.42, Issue 3, pp. 207-215.
- YU L., XUE M.-A., JIANG Z. (2020a). Experimental investigation of parametric sloshing in a tank with vertical baffles, *Ocean Engineering*, Vol.213, Paper ID 107783.
- YU L., XUE M.A., ZHENG J. (2019). Experimental study of vertical slat screens effects on reducing shallow water sloshing in a tank under horizontal excitation with a wide frequency range, *Ocean Engineering*, Vol.173, pp. 131–141.
- YU L., XUE M.A., ZHU A., (2020b). Numerical Investigation of Sloshing in Rectangular Tank with Permeable Baffle, *Journal of Marine Science and Engineering*, Vol.8, Issue 9, Paper ID 671.